Atmospheric Environment 43 (2009) 6091–6099

Contents lists available at ScienceDirect

Atmospheric Environment

journal homepage: www.elsevier.com/locate/atmosenv

Three-dimensional characterization of the ammonia plume from a beef cattle feedlot

Ralf M. Staebler [a,*], Sean M. McGinn [b], Brian P. Crenna [c], Thomas K. Flesch [c], Katherine L. Hayden [a], Shao-Meng Li [a]

[a] Science & Technology Branch, Environment Canada, Toronto, ON, Canada
[b] Agriculture and Agri-Food Canada, Lethbridge, AB, Canada
[c] University of Alberta, Edmonton, AB, Canada

ARTICLE INFO

Article history:
Received 27 November 2008
Received in revised form
4 August 2009
Accepted 5 August 2009

Keywords:
Ammonia
Beef feedlot emissions
Airborne measurements
Local ammonia budget
Backward Lagrangian stochastic model
Alberta

ABSTRACT

In Canada approximately 45% of ammonia (NH_3) emissions are attributed to dairy and beef cattle industries. The present study focused on NH_3 emissions from a beef feedlot with a one-time capacity of 17,220 head. The aim was to improve the Canadian NH_3 emission inventories and air quality forecasting capabilities. A Cessna 207, equipped with a fast-response NH_3/NO_y detector and a quadrupole aerosol mass spectrometer, was flown in a grid pattern covering an area of 8 × 8 km centered on a feedlot (800 × 800 m) at altitudes ranging from 30 to 300 m above ground. Stationary ground measurements of NH_3 concentration and turbulence parameters were made downwind of the feedlot. Three flights were conducted under varying meteorological conditions, ranging from very calm to windy with near-neutral stratification. NH_3 mixing ratios up to 100 ppbv were recorded on the calm day, up to 300 m above ground. An average feedlot NH_3 emission rate of 76 ± 4 μg m^{-2} s^{-1} (equivalent to 10.2 g $head^{-1}$ h^{-1}) was estimated. Characteristics of the measured NH_3 plume were compared to those predicted by a Lagrangian dispersion model. The spatially integrated pattern of NH_3 concentrations predicted and measured agreed but the measured was often more complex than the predicted spatial distribution. The study suggests that the export of NH_3 through advection accounted for about 90% of the emissions from the feedlot, chemical transformation was insignificant, and dry deposition accounted for the remaining 10%.

1. Introduction

Overlying the increasing pressure on agriculture to produce food for an increasing global population, there is an expectation that agriculture needs to reduce emissions of pollutants to the atmosphere. A priority for research is to quantify the emission, transport, transformation and deposition of pollutants from agriculture. Aneja et al. (2006) succinctly phrased, "There is just enough information for researchers and policy makers to recognize a serious problem (of agricultural pollutants), but not enough information for them to understand the extent of the problem or to make scientifically credible recommendations about potential solutions, which may ultimately influence air, soil and water quality, human health, and the economy of agricultural regions."

Agriculture accounts for more than 96% of all anthropogenic emissions of atmospheric NH_3 (Isermann, 1994), mainly from livestock manure and urea fertilizers (Environment Canada, 2009). The NH_3 emission rate from these sources and downwind concentration depend on meteorological conditions, the type of manure and its management, and the form and placement of inorganic fertilizer. In the case of land applied manure or inorganic fertilizers, time and rate of application, and soil condition (pH, moisture, and temperature) also influence emission (Environment Canada, 2009).

The important role of agriculture in the atmospheric NH_3 budget can be seen in the relationship between NH_3 concentration and proximity to livestock operations. Typical continental concentrations of atmospheric NH_3 are between 1 and 10 μg m^{-3} (Lemon and van Houtte, 1980; Ryden and McNeill, 1984; Wollenweber and Raven, 1993), equivalent to a mixing ratio of 1.3–13 ppbv at standard temperature and pressure. Adjacent to a 25,000 head feedlot, McGinn et al. (2003) reported NH_3 mixing ratios near the ground in excess of 4600 ppbv, decreasing to 460 ppbv just 200 m downwind. Regional concentrations in the vicinity of intensive feedlot operations were 90–130 ppbv. Luebs et al. (1974) measured NH_3 concentrations of 700 ppbv at 800 m downwind of a corral

* Corresponding author.
E-mail address: ralf.staebler@ec.gc.ca (R.M. Staebler).

1352-2310/$ – see front matter
doi:10.1016/j.atmosenv.2009.08.045

containing 600 cattle. Allen et al. (1988) reported that mixing ratios of NH_3 in an area with livestock farms were between 26 and 38 ppbv, several times higher than at sites without livestock.

Some of the emitted NH_3 is deposited back to the nearby downwind surfaces. Deposition of NH_3 was reported to be 68 and 32 kg N ha^{-1} yr^{-1} at distances of 75 and 700 m downwind of a poultry barn, respectively (Berendse et al., 1988). In Canada, data of McGinn et al. (2003) showed annual NH_3 deposition to dry soil between 29 and 41 kg N ha^{-1} adjacent to an intensive livestock operation. NH_3 that is not deposited immediately from the atmosphere can react with nitric or hydrochloric acid to form reversible NH_4NO_3 and NH_4Cl (Allen et al., 1988). However, over eastern North America the predominant sink of NH_3 in the atmosphere is the reaction with acidic sulphate aerosols forming $(NH_4)_2SO_4$ and NH_4HSO_4, and the uptake of NH_3 in clouds and precipitation. The majority of the NH_3 emitted is eventually deposited back to the surface through wet deposition (Krupa, 2003).

In contrast to the variability in NH_3, concentrations of aerosol NH_4^+ are spatially more uniform because it is more stable and transported over longer distances. Once formed, aerosol NH_4^+ is removed from the atmosphere by dry and wet deposition. Background concentrations of aerosol NH_4^+ range between 1 and 3 μg m^{-3} and NH_4^+ concentrations in rainwater are on the order of 20 μmole L^{-1} (van der Eerden, 1982). Where livestock is prevalent in a region, the rainwater concentration is reported close to 100 μmole L^{-1} (van der Eerden, 1982). Even higher concentrations, on the order of 2000 μmole L^{-1}, were reported under a forest canopy (Roelofs et al., 1985). In Alberta, concentrations of NH_4NO_3 and $(NH_4)_2SO_4$ were reported to range from 0.1 to 0.4 and 0.03 to 0.21 μg m^{-3}, respectively (Cheng and Angle, 1996).

The manure associated with raising beef cattle is responsible for about 32% of the Canadian NH_3 emissions, and operations in Alberta accounts for half of these emissions (16%) (Environment Canada, 2009). The typical size and internal heterogeneity of beef feedlots suggest that micrometeorological techniques are best suited to determine representative average emission rates (McGinn et al., 2007). A suitable approach is the backward Lagrangian stochastic (bLS) model used to derive upwind emission source strengths from measurements of concentrations and micrometeorological parameters downwind of the source (Flesch et al., 1995, 2007). This method has been verified using a tracer approach (McGinn et al., 2006) and surface layer profiles measurements (Sommer et al., 2004; Laubach and Kelliher, 2005).

In this paper, airborne measurements are used to examine the capacity of the bLS backward Lagrangian stochastic model to predict the characteristics of the NH_3 plume emanating from a beef feedlot near Lethbridge, Alberta. The results provide much needed information on the vertical distribution of NH_3 in the boundary layer (Georgii and Müller, 1974; Ziereis and Arnold, 1986; Beig and Brasseur, 2000), and address the question on how to upscale emissions from the feedlot scale to that of air quality models (cf. Zhang et al., 2002). The first goal of this study is to generate estimates of the local net emission rate and emission factor to improve the national NH_3 emission inventory. Secondly, the results should improve the characterization of sub-grid-scale dispersion and transformation of NH_3 to account for these processes in the national air quality models.

2. Experimental methods

Located in southern Alberta, Canada, Lethbridge County has one of the highest cattle densities in Canada with approximately 600,000 head of cattle (Toma and Bouma Management Consultants, 2006). Measurements were made at and around a beef feedlot near Enchant (50.15°N, 112.36°W) in Lethbridge County. At the time of our study, the feedlot contained approximately 17,220 beef cattle (primarily Angus and cross breeds) in adjacent pens covering an area of 800 by 800 m. The cattle typically enter the feedlot weighing about 350 kg and gain weight on a high grain diet (1.4 kg d^{-1}) over a 130 day period. The source of NH_3 from this facility will be the urine and feces excreted by the cattle. The manure pack that builds up in the cattle pens is typically removed from the feedlot twice a year. At the time of this study, pen cleaning was initiated and was expected to result in slightly higher than normal NH_3 emissions.

On the ground, NH_3 concentration was measured with an open-path laser (Boreal Lasers, Model GasFinder) using a path parallel to the eastern edge of the feedlot at a distance of 155 m, and a path length of 527 m at a height of 1.5 m above ground (Fig. 1). A sonic anemometer (SATI/3Sx, Applied Technologies Inc., Colorado), co-located with the laser, provided wind and turbulence data at 2 m above ground. More details can be found in McGinn et al. (2007), describing a similar field study at the same site in 2006.

Airborne measurements were performed from a Cessna 207 aircraft customized for air quality studies. Ammonia was measured with an analyzer that converts total reactive nitrogen (N_t) and NO_y to NO by passing the sampled gas through high-temperature catalytic converters (650 °C for N_t, 325 °C for NO_y) and then detects the NO through its chemiluminescent reaction with O_3 (CLD 88 CYpr, Eco-Physics AG, Switzerland). NH_3 is calculated as the difference between N_t and NO_y, although this may include an unknown fraction of amines that may also be converted by the 650 °C converter. The RMS noise between 4-s samples was typically 0.1 ppbv for N_t and NO_y, resulting in 0.14 ppbv for NH_3.

An inlet for air sampling was mounted 50 cm above the center of the wings, above the slipstream of the propeller. The air was pumped at 25 L min^{-1} through a ¼″ (0.48 cm ID), 3.5 m Teflon tube and a sub-sample of this air (at 1.2 L min^{-1}) was diverted into the instrument through a 1/8″ Teflon tube (0.16 cm ID, 0.3 m length).

Calibrations were performed through an identical sample line, with known standards of NO (Scott-Marrin, Riverside, CA) and permeation tubes for NH_3 (Vici Metronics Inc., Poulsbo, WA),

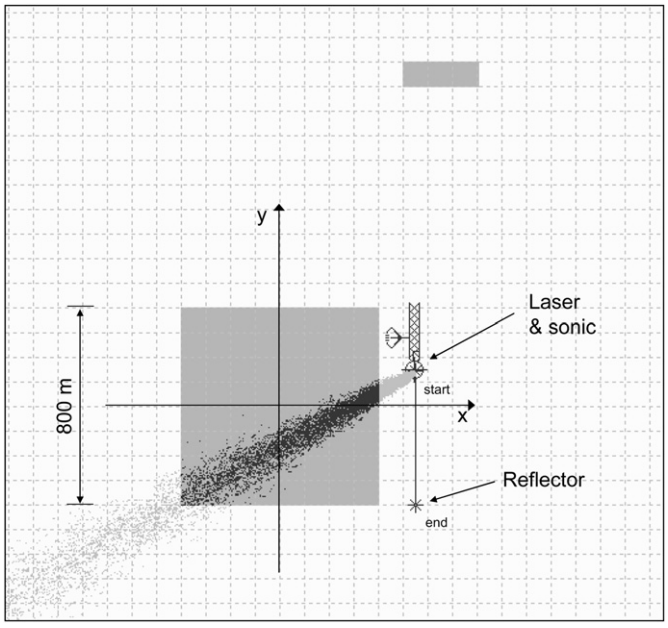

Fig. 1. Map of the feedlot and the ground-based measurements on the eastern edge. Also shown is an example of the "touchdowns" generated by the bLS model, for a south-westerly wind direction and near-neutral conditions. Feedlots are shown in grey.

diluted with zero air using a Dynamic Gas Calibration System (Model 146, Thermo Environmental Instruments Inc., Franklin, MA). The calibrations consistently indicated that passing NO through the 650 °C converter produced a signal 15.4% lower than the 325 °C converter, most likely due to NO being oxidized to NO_2 at the higher temperature and therefore not being detected in the chemiluminescent process. This was factored into the calibration to produce the final concentrations.

The response time of the system (i.e., the 10–90% rise time upon receipt of a step concentration change) was 10 s with a delay of about 30 s. The spatial resolution of the aircraft measurements, at a typical ground speed of 50 m s^{-1}, was therefore 500 m.

A Quadrupole Aerodyne Aerosol Mass Spectrometer (Q-AMS) was used to measure the aerosol composition including nitrate, sulphate, organics and ammonium at 2 min intervals. Details of the Q-AMS have been described previously (Jayne et al., 2000; Allan et al., 2003; Jimenez et al., 2003; Hayden et al., 2008). Ambient particles less than ~1 μm in diameter are sampled through a critical orifice, focussed into a narrow beam and then directed onto a heated surface (550 °C) where non-refractory chemical constituents are flash vapourized. The vapour is ionized by electron impact and the resulting fragments analyzed by a quadrupole mass spectrometer.

3. The Lagrangian model

A backward Lagrangian stochastic (bLS) model (Flesch et al., 1995) was used for three purposes: i) to estimate the emission rate of the feedlot based on concentrations measured downwind of the feedlot on the ground; ii) to estimate the feedlot emission rate based on the concentration measurements from the aircraft; and iii) to predict the spatial characteristics of the plume given the estimated the NH_3 emission rate.

The bLS model calculates atmospheric transport by simulating the paths of passive tracer particles as they move through the atmosphere. Each path is unique due to a random component of the particle motion, which simulates the effect of atmospheric turbulence. Model calculations of average tracer concentrations are based on the ensemble of trajectories. WindTrax is a surface layer model, depicting transport in the lowest 100 m (approximately) of the atmosphere, where Monin–Obukhov similarity relationships describe the statistical properties of the wind. Model details are given in Flesch et al. (2005).

The first use of the bLS model is to provide inverse-modelling of emissions: surface NH_3 concentrations downwind of the feedlot are used to derive an NH_3 emission rate. The feedlot is described as a collection of surface sources corresponding to the cattle pens, with an assumed spatially uniform emission rate of NH_3. The relationship between concentration and emission rate is calculated by simulating the transport of NH_3 from the pen surfaces to the downwind concentration sensor under the measured wind conditions. As input, the bLS model requires a map of the feedlot/sensor layout, average wind and turbulent information, and concentration observations. The model is used to calculate emissions from 15-min concentration and wind averages. This technique has been successfully used to calculate feedlot emissions in other studies (Flesch et al., 2007; McGinn et al., 2007). Similarly, a second estimate of the feedlot emission rate is calculated based on the aircraft concentration data.

The third application of the bLS model is to extrapolate from the calculated feedlot emission rates to the downwind NH_3 concentration fields. This allows a comparison of the aircraft observations with model output. The use of a bLS model designed for the surface layer, and the assumption of horizontally homogeneous atmosphere may limit the accuracy of the extrapolation. Given that the observations extend some distance above and downwind of the feedlot, it may be sensitive to ignoring the above-surface layer details of the atmosphere. For example, Flesch et al. (1995) suggests a surface layer model is adequate for distances less than about 1 km downwind of a surface source. Ignoring the inhomogeneous nature of winds around the feedlot (cf. Flesch et al., 2007) reduces the accuracy of the model calculations further downwind and aloft. Thus the bLS calculations downwind of the feedlot represent idealized conditions, and are subject to a level of uncertainty larger than found in smaller scale bLS applications. It is also worth noting that a more rigorous treatment of atmospheric transport in this real world case would be dramatically more demanding and beyond the capabilities of this study.

This version of the bLS model does not incorporate any deposition or chemical processes. It assumes that NH_3 emitted from the feedlot is a passive tracer. The differences between the model and the actual observations may therefore be a measure of the importance of these processes relative to turbulent dispersion.

4. Observations

Three flights were conducted over the feedlot between 14 and 29 September 2005. Winds during Flight 1 were light (less than 2 m s^{-1}) and the direction erratic, and in combination with a significant heat flux resulted in nearly free convection conditions (Table 1). The small, negative Obukhov length (L) indicates an unstable stratification. Flight 3 was marked by high wind speeds from the southwest, a smaller heat flux and a much larger (negative) L, signifying close to neutral stratification. Conditions for Flight 2 were between these two extremes, although they were closer to neutral than unstable. The daytime unstable and near-neutral conditions are associated with deep surface layers, which should increase the accuracy of the surface-layer bLS simulations (in both downwind and vertical directions) compared with stable or nighttime cases.

Based on 15-min averages of NH_3 concentrations and corresponding measurements of wind statistics (Table 1), the bLS model was used to estimate emission rates from the feedlot. Since wind speeds were low and wind directions erratic during Flight 1 (conditions known to be associated with dispersion model inaccuracies), this was only done for Flights 2 and 3 which had consistent winds from the feedlot towards the long-path NH_3 sensor. The surface roughness length as determined by the downwind sonic anemometer (median 0.06 m) was used in the bLS model runs. A constant background NH_3 mixing ratio was subtracted beforehand, based on a spatial average of NH_3 upwind of the feedlot (7 and 10 ppbv for Flights 2 and 3 respectively). During Flight 2, the mean and standard deviation of the emission rate was

Table 1
Average meteorological ground conditions during the three flights. Standard deviations are given in parentheses. U is the mean wind, u_* the friction velocity, and L the Obukhov length, based on sonic anemometer measurements at 2 m above ground, 155 m east of the feedlot. Times are Mountain Daylight Savings Time. Also given is the mean NH_3 mixing ratio 155 m east of the feedlot.

	Flight 1 20 Sept 05 10:00–13:00	Flight 2 25 Sept 05 15:00–19:00	Flight 3 26 Sept 05 13:00–16:00
U (m s^{-1})	1.38 (0.44)	2.42 (0.52)	7.7 (1.1)
Wind direction	350 (146)	231 (23)	215 (22)
u_* (m s^{-1})	0.26 (0.08)	0.30 (0.07)	0.76 (0.08)
Sensible heat flux (W m^{-2})	153 (64)	58 (68)	51 (42)
L (m)	−6.4 (8.2)	−81 (32)	−887 (867)
T (°C)	13.7 (2.0)	19.0 (1.0)	21.4 (0.4)
[NH_3] (ppbv)	97 (63)	238 (83)	177 (37)

64 ± 4 μg NH_3 m^{-2} s^{-1} (15 15-min periods), and during Flight 3 it was 88 ± 5 μg m^{-2} s^{-1} ($n = 11$), where the uncertainty represents the statistical uncertainty of the bLS output. These rates extrapolate to 8.5 and 11.8 g $head^{-1}$ h^{-1}, or 148 and 203 kg h^{-1} for the whole feedlot during Flights 2 and 3, respectively. The emission rate used for Flight 1 was an average of the other two flights (75 μg m^{-2} s^{-1}). These emission rates are about 10% lower than mid-day emissions observed a year later, 84 μg m^{-2} s^{-1}, at the same feedlot with a higher cattle density of 22,500 (McGinn et al., 2007), using in-feedlot rather than downwind measurements.

The "touchdown fraction" calculated by the bLS model is an estimate of the fraction of the feedlot surface "sampled" by the downwind laser (a higher value means more of the feedlot is contributing to the laser concentration, which should lead to a more representative measurement). This fraction was on average 28%, a reasonably high value (Flesch et al., 2007).

These emission rates were used in combination with the meteorological data as input to the bLS model in predictive runs to compare with the aircraft measurements. Horizontal planes at various altitudes above the surface, covering an area of 8 × 8 km

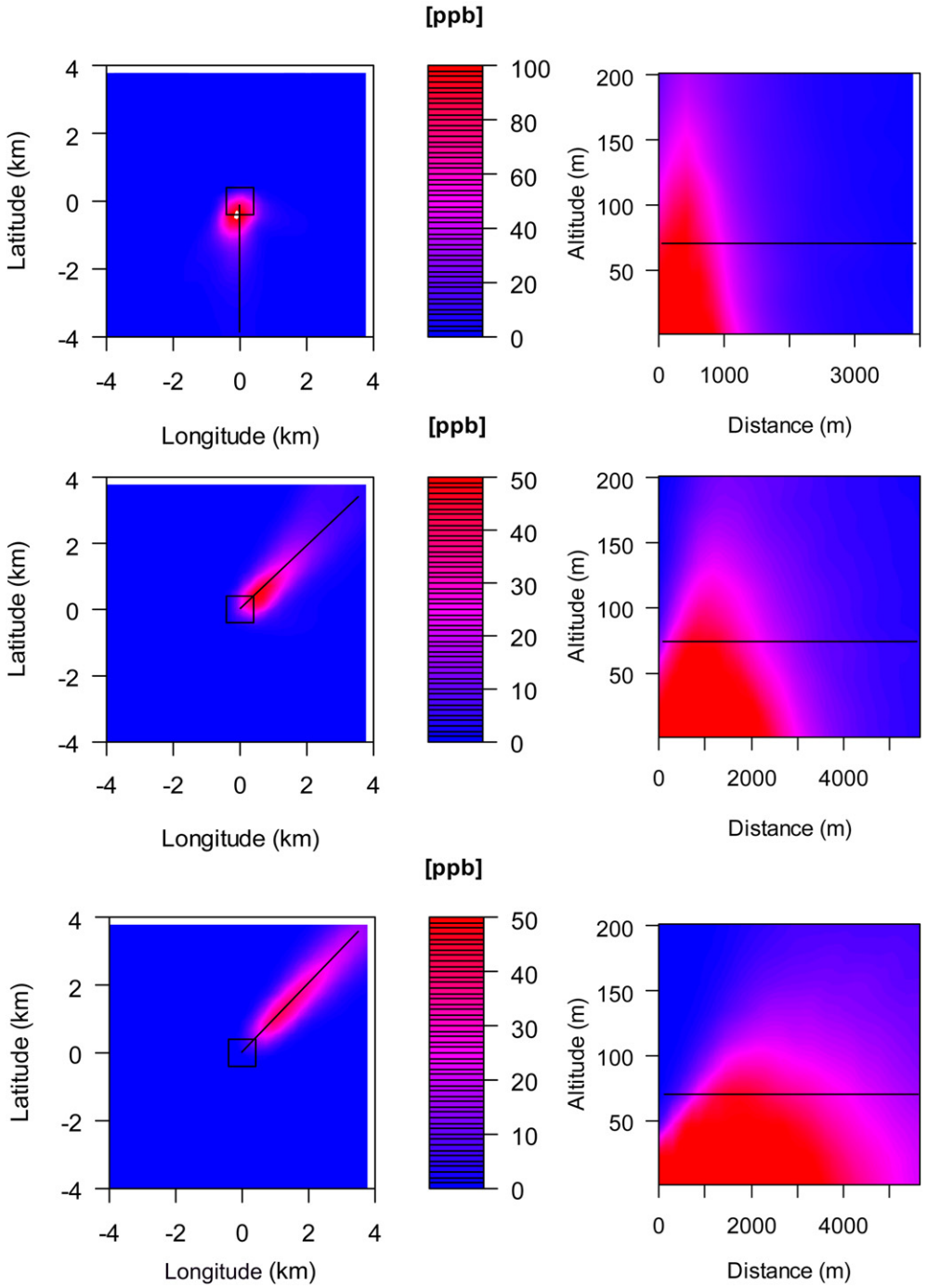

Fig. 2. Color NH_3 contour plots for Flights 1, 2 and 3, based on the bLS model output. The left column displays "downward looking" horizontal contours at 75 m above ground, the right column "sideways looking" vertical profiles. The black line in the horizontal plot indicates the location of the cross section for the vertical plot, and the horizontal black line in the vertical plots indicate the altitude of the cross section for the horizontal plots. Note that the scale for Flight 1 is different from the other two.

centered on the feedlot, were specified as the sensor surfaces in the software, and the NH_3 concentration at 1600 grid points at these altitudes (spaced 200 m apart) was estimated for each 15-min period. To provide a side view of the plume, the concentrations along vertical slices was also calculated. The predicted average plume, timed to the 15-min averages of Flight 1, was confined to the area immediately south of the feedlot, peaking at the southern edge and extending for about 1 km (Fig. 2). Mixing ratios slightly greater than 80 ppbv at altitudes up to 120 m were predicted. During Flight 2, a persistent south-west wind averaging 2.4 m s^{-1} resulted in the plume extending towards the north-east, with mixing ratios up to 50 ppbv predicted at 2 km downwind at 75 m above ground. Flight 3, with relatively strong winds (averaging 7.7 m s^{-1}) from the same direction, stretched this plume farther, predicting almost 50 ppbv 3 km downwind at 75 m above ground.

These results were then compared to the aircraft data (Fig. 3), after interpolating to the same scale (Fig. 4). Only flight data at levels of 75 ± 25 m were used to construct the bilinear interpolation onto a plane of grid with a 200 m spacing, which is a higher resolution than the expected instrumental spatial resolution, but does allow for easier identification of the tracks that contributed to the plot.

On Flight 1, NH_3 up to 100 ppbv was measured, surprisingly not at the lowest flight altitude (30 m), but 60 m above ground. This may be explained by temporal or spatial fluctuations that are not captured by the aircraft measurements. The highest concentrations were found within 300 m to the south-west of the feedlot. The bLS model predicted higher mixing ratios (around 80 ppbv) than observed at the 75 m altitude during the flight, and the observations showed the plume extending farther to the south-west. The NH_3 mixing ratio at 30 m above ground, away from the feedlot, was relatively high at ~15 ppbv on this day.

On Flight 2, levels up to 80 ppbv were observed at 30 m; the highest levels were found at a distance of ~1 km to the NE of the lot. The location and magnitude of the NH_3 maximum predicted by the bLS model agree well with the observations. On this day, the NH_3 levels away from the feedlot at the 30 m level were around 3 ppbv.

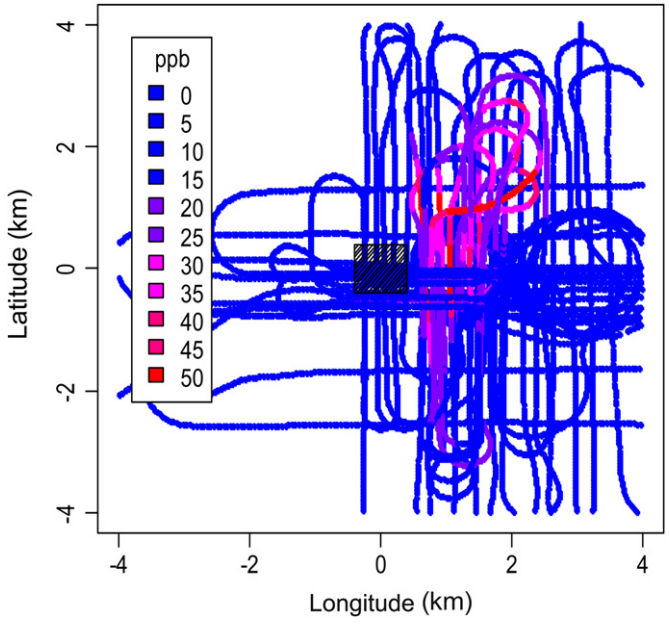

Fig. 3. The flight path for 25 Sept 2005. The color of the trace is a function of the NH_3 mixing ratio. The origin of the coordinate system is the center of the feedlot, which is marked by a shaded square. Note that flight tracks at all altitudes are shown.

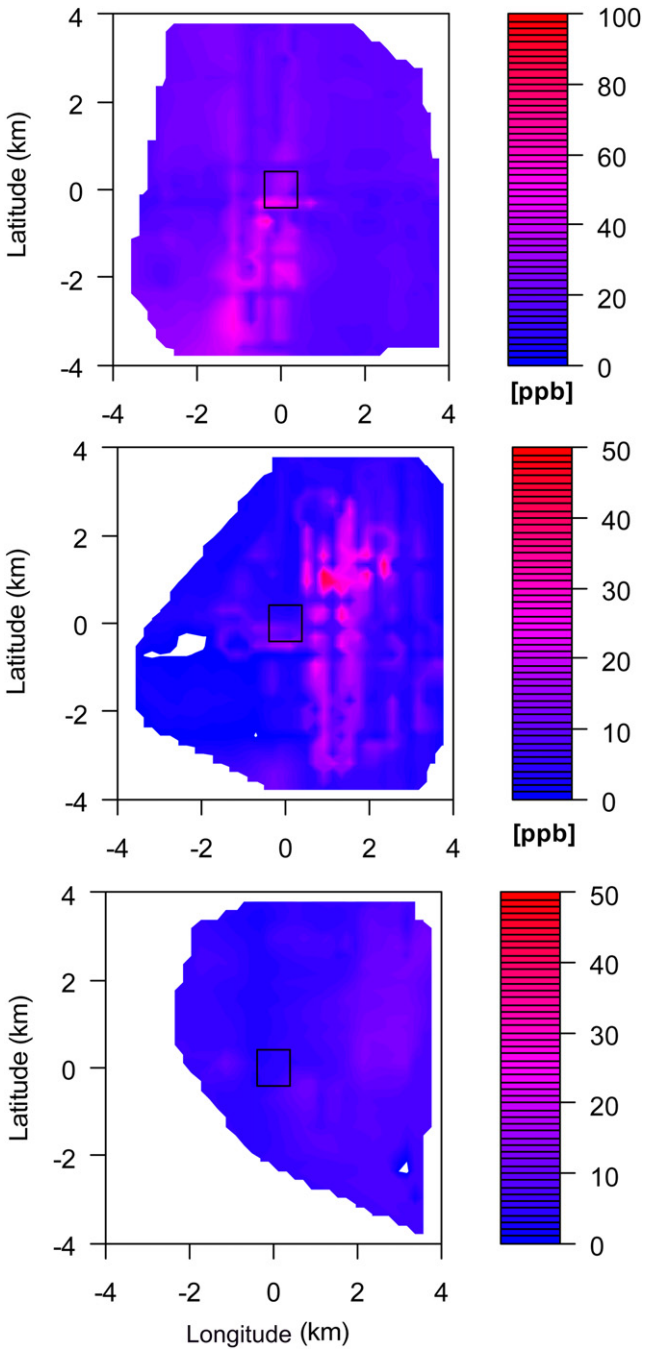

Fig. 4. Observed NH_3 mixing ratios at 75 m above ground for Flights 1, 2 and 3 (a, b, c respectively). The plot is constructed using bilinear spline interpolation from the track data (cf. Fig. 3) onto a 200 m grid.

On Flight 3, even at levels 30 m over the feedlot, NH_3 was never higher than 25 ppbv. Similar to Flight 2, the maximum was found ~1 km to the north-east. The NH_3 levels away from the feedlot on this day were around 10 ppbv. In the layer from the surface to 75 m, the bLS model predicted higher mixing ratios (50 ppbv) than observed at any level during this flight.

5. Discussion

In Fig. 5, average vertical profiles of NH_3 from the aircraft measurements and bLS model predictions are compared for Flights

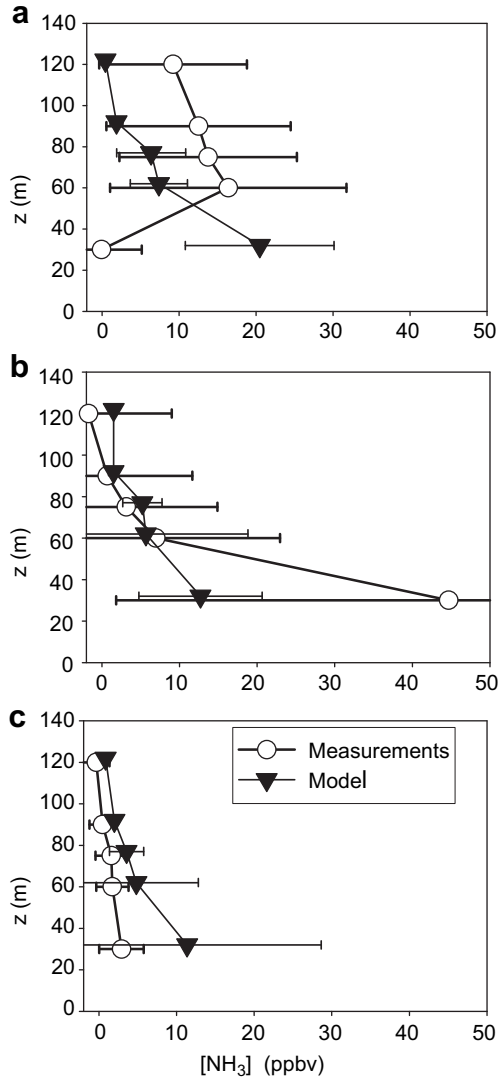

Fig. 5. Vertical NH_3 mixing ratio profiles for Flights 1, 2 and 3. The dashed line denotes the bLS model, the solid line the measurements. Horizontal lines denote population standard deviations.

1–3. The area averaged was adjusted according to the position of the NH_3 plume; for Flight 1, this corresponded to -1 km < Longitude < 1 km and -4 km < Latitude < 0 km (the origin being the center of the feedlot). For Flights 2 and 3 the whole north-east quadrant (i.e., 0 km < Longitude < 4 km, the same for Latitude) was averaged. The flight data were averaged into horizontal slabs centered on 30, 60, 75, 90 and 120 m, corresponding to the levels used in the bLS model. The upwind mixing ratio in the immediate vicinity of the feedlot was subtracted from the observational data for each flight before comparison, since it represents NH_3 advected into the area, and therefore would not be predicted by the model. For Flight 1, the highest NH_3 levels measured from the aircraft were at altitudes 60 m and higher, whereas the model predicted a monotonic decrease with height. This elevated maximum is difficult to explain, but probably reflects the limited horizontal extent of the plume at lower levels under the free convection conditions on this day, and that the aircraft apparently missed the highest concentrations expected right over the feedlot because of spatial or temporal variability of the emissions. For Flight 2, higher concentrations were observed than predicted at the 30 m level, but there is good agreement at higher altitudes. In Flight 3, observed NH_3 concentrations were consistently lower than model concentrations, but within the range of observations denoted by the horizontal error bar at each level.

The agreement between measured and modelled results was tested using volume integrals of the total amount of NH_3 in the air volume above and downwind of the feedlot, after subtracting the background mixing ratios from the observations as described for Fig. 5. During the unstable conditions of Flight 1, there was almost twice as much NH_3 for measured results compared to the modelled results when integrated out to a distance of 4 km from the center of the feedlot (Fig. 6). This suggests that the erratic, almost stagnant wind conditions kept previously emitted plumes in the volume much longer than constant, monotonic diffusion. For Flight 2, the measured and modelled volume integrals agreed well (slope = 1.2, $r^2 = 0.99$), especially further away from the feedlot. For Flight 3, the total amount of NH_3 measured was 45% below the modelled value. A possible explanation is that during these windy conditions, the downwind anemometer was in a slower flow regime due to shading by the feedlot, and if this is extrapolated up over the whole domain, the emissions are less diluted in the model than they would be by the real, faster ambient flow. In other words, the slower modelled flow advects the feedlot emissions more slowly away and therefore dilutes them less than the actual faster flow aloft.

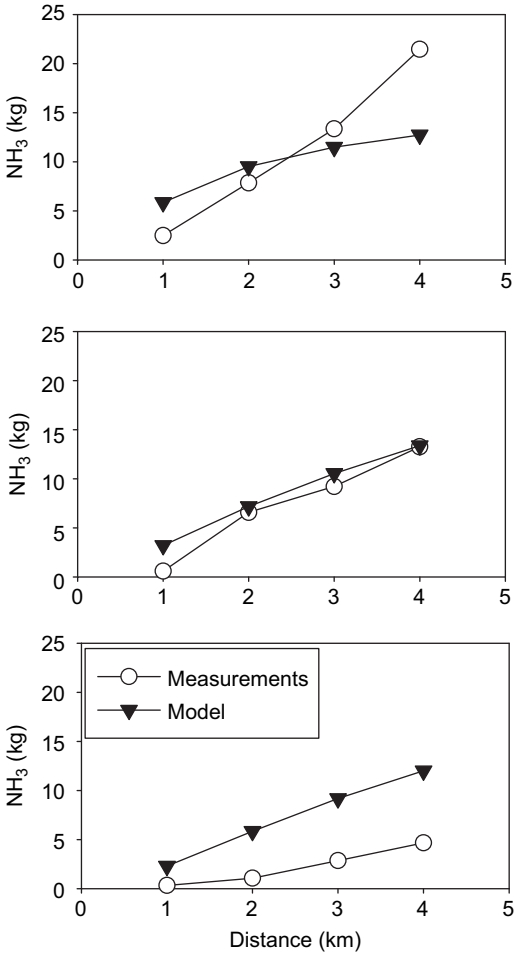

Fig. 6. Accumulated NH_3 as function of distance from the feedlot center. The total amount of NH_3 in the air mass from 0 to 135 m above ground, and covering a square that extends the distance shown on the *x* axis from the center of the feedlot, is shown. The solid line denotes measurements, the dashed line the bLS model.

The emission rates for the feedlot may also be derived from the NH_3 mixing ratios measured on the aircraft. For this, again only Flights 2 and 3 were used because of their better defined boundary layer conditions. The emission estimates obtained this way were strongly dependent on the threshold of the minimum touchdown fraction for each 4-second data point included in the average, and to the threshold for allowable noise in the emission estimate. Requiring touchdown fractions above 20% reduced the emission estimate from an average of 84 $\mu g\ m^{-2}\ s^{-1}$ to below 30 $\mu g\ m^{-2}\ s^{-1}$. Similarly, a minimum relative standard deviation of less than 0.5 decreased the emission estimate to below 34 $\mu g\ m^{-2}\ s^{-1}$, but as the threshold was relaxed to above 1.5, the emission estimate asymptotically approached 84 $\mu g\ m^{-2}\ s^{-1}$.

This large variability is caused by the fact that measurements near the edge of the plume produced high emission estimates, and those near the center of the plume relatively low estimates. This indicates a mismatch between the observed lateral plume dispersion from that in the model. Relaxing the thresholds and including a larger fraction of the measurements asymptotically improves the estimates, by making the exact shape of the plume irrelevant. The average emission estimate obtained this way (84 $\mu g\ m^{-2}\ s^{-1}$) agrees well with the ground-based estimate (75 $\mu g\ m^{-2}\ s^{-1}$), but with a much larger uncertainty (115 vs. 5 $\mu g\ m^{-2}\ s^{-1}$) due to the fact that on average only 8% of the flight time was spent in the feedlot plume (defined by a nonzero touchdown fraction).

Since the bLS model used in this study did not account for deposition or chemical transformations, the difference between the observations and model predictions can theoretically be used to assess the relative magnitude of these mechanisms compared to dispersion. However, there are practical limitations to this comparison: first, the aircraft does not measure the whole volume instantaneously, and therefore, the interpolated NH_3 fields discussed earlier are interpolations both in space and time; and secondly, since only 2–3 altitudes could be flown in a flight, points may only represent transitions between altitudes. The reasonably good agreement between model and observations suggests that the dominant mechanism determining the spatial distribution and concentration of NH_3 is indeed turbulent dispersion, and that deposition and chemical transformations are secondary factors.

The predominant chemical loss of NH_3 in Southern Alberta is expected to be the reaction with HNO_3 to form NH_4NO_3 in aerosols, and by uptake of NH_3 on pre-existing aerosols. The Q-AMS measured typical aerosol NH_4^+ concentrations of $<0.7\ \mu g\ m^{-3}$ at any altitude for Flights 2 and 3, or <1.1 ppbv mixing ratio at the typical 20 °C and 850 hPa. Most of this aerosol NH_4^+ was in the background aerosols advected into the flying area. Thus the chemical loss of NH_3 through local NH_3-aerosol chemistry would be much less than 1 ppbv and insignificant compared with dilution through turbulent mixing in the volume of air impacted by the emissions. In Flight 1, mass concentrations were higher with NH_4^+ and NO_3^- peaking at 1.6 and 5 $\mu g\ m^{-3}$, respectively. The chemical losses of NH_3 were relatively more significant in Flight 1 compared to the other flights, and were consistent with the more stagnant boundary layer conditions and therefore increased residence time in the volume, allowing more time for chemical reactions to take place.

The rapid decrease of NH_3 concentration with distance from a strong source should not be misconstrued as evidence of significant dry deposition of NH_3. It is shown here that even in the absence of chemistry or deposition, drastic decreases in concentration with distance from the source are predicted, entirely due to turbulent mixing and dilution. In Fig. 7, the output from the bLS model for Flight 2 clearly shows NH_3 mixing ratios at 1 m above ground dropping by 2 orders of magnitude over a distance of 3 km even along the main wind vector (north-east), and more than two orders of magnitude over just 1 km from the edge of the feedlot at a 45° angle to the wind vector (east). In fact, a low of 0.2 ppbv, the detection limit of the instrument, is reached less than 3 km from the feedlot. In the real atmosphere, a regional background concentration of NH_3 will be found that is significantly higher, determined by a balance of emissions on a regional scale with advection, deposition and chemical transformation.

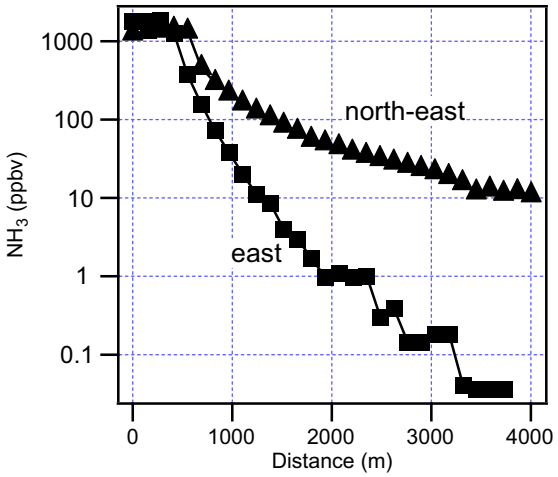

Fig. 7. NH_3 mixing ratios predicted by the bLS model along transects 1 m above ground, starting from the center of the feedlot, along the wind vector (north-east) and at 45° from it (east).

The magnitudes of the NH_3 budget components are estimated to elucidate their relative significance. The 8 × 8 km × 135 m volume, discussed earlier, contains on the order of 10 kg of NH_3 (Fig. 6). This, combined with a feedlot emission rate of 2 kg min^{-1}, yields a crude residence time estimate of 5 min. With typical wind speeds of 3 m s^{-1}, this corresponds to an advection distance of 900 m. The advection out of the volume, across a plane perpendicular to the wind direction at a distance of 4 km from the feedlot up to an elevation of 135 m, is on the order of 0.2–0.7 kg min^{-1}, based on simulations with the bLS model. Using a deposition velocity for NH_3 of 1 cm s^{-1} (Zhang et al., 2002), the magnitude of deposition can be estimated. Multiplying the spatial NH_3 distribution predicted with the bLS model at 1 m above the surface by this deposition velocity, a rough estimate of the dry deposition is 0.12–0.24 kg NH_3 min^{-1} from the volume onto the 8 × 8 km square, i.e., about 10% of NH_3 emitted from the feedlot. This is in good agreement with the prediction by Fowler et al. (1998) of 10% of NH_3 deposited within 1.2 km of a chicken farm. Using the current calculated deposition estimate, an average of 2.9 mg $m^{-2}\ h^{-1}$ of NH_3 is deposited within the first 400 m of the feedlot, which agrees in magnitude with observations published previously (McGinn et al., 2003). As shown earlier, chemical conversions on this spatial and temporal scale are insignificant. Therefore the remainder (1.1–1.7 kg min^{-1}) must be transported to levels above 135 m within the first 4 km from the source, presumably to be transported out of the volume through horizontal advection between 135 m and the top of the boundary layer. As previously discussed, there is a large uncertainty in these calculations made using this surface-layer bLS model, given the relatively large spatial domain of our application.

6. Summary

A study of NH_3 emissions from a beef feedlot in Southern Alberta in 2006 revealed mid-day emission rates between 64 ± 4 and 88 ± 5 $\mu g\ m^{-2}\ s^{-1}$ of NH_3, based on downwind NH_3 and turbulence

measurements applied to a bLS model. This extrapolates to 8.5 (11.8) g head^{-1} h^{-1}, or 148 (203) kg h^{-1} for the whole feedlot respectively. Using aircraft NH_3 measurements, an average emission rate of 84 $\pm$ 115 μg m^{-2} s^{-1} was calculated, confirming the ground-based results. The integrated feedlot emission rate compares well with that found by McGinn et al. (2007) a year later at the same site (131 kg h^{-1}), although cattle density was much higher in 2006 (22,500 vs. 17,220 in 2005). The reason for the higher per capita emissions may be that the 2005 measurements were taken just before pen cleaning operations. The higher emission rate estimate for the third flight day may be due to the strong winds on this day, resulting in a highly turbulent wake downwind of the feedlot and an overestimation of the vertical diffusion by the bLS model.

Direct NH_3 measurements on an aircraft, with a spatial resolution that is useful to study the emission plume from a point source, are now feasible with fast-response chemiluminescence analyzers. On 3 separate days over different meteorological conditions, the plume was mapped in 3 dimensions and compared with the plume dimensions and concentrations predicted by the surface-layer bLS model. For the calm first flight, mixing ratios up to 100 ppbv were encountered, and much residual NH_3 was observed that was not clearly linked with the feedlot. NH_3 observations were consistently higher at elevations above 50 m than predictions, while flight tracks at the lower elevations apparently missed the highest concentrations due to the spatial and temporal variability of the emissions. On the second flight with moderate winds and near-neutral stratification, good agreement was found between model and observations at elevations above 50 m. The third flight, on a windy day, produced observations consistently lower than those predicted. The integrated mass of NH_3 for a volume of 8 $\times$ 8 km $\times$ 135 m centered on the feedlot as predicted by the model was similar in all three scenarios, but varied significantly in the measurements. On the first (calm) flight, the observed mass was a factor of almost 2 larger than the model, for the second flight it agreed within 10% for distances >1 km, and on the third flight it was lower by a factor of >2.

The bLS model predicts the observed plume well under conditions of near-neutral thermal stratification and moderate winds, but has trouble with conditions associated with free convection or strong winds. Under calm conditions, the spatial distribution of NH_3 is confounded due to emitted plumes stagnating and re-circulating, in addition to elevated background levels due to surrounding feedlots. Under strong winds, the wake of the feedlot with its greater roughness length than the surrounding fields may result in an overestimate of the feedlot emissions and exaggerated vertical dispersion of the plume.

An estimate of the budget for a volume centered on the feedlot with dimensions 8 $\times$ 8 km $\times$ 135 m suggests that 10–35% of the NH_3 emitted by the feedlot leaves the volume at elevations between the ground and 135 m, 50–80% leaves the surface layer vertically, dry deposition accounts for 6–12%, and chemical transformation is insignificant.

Considering the expected variability among feedlots, seasonal variations within one feedlot, and different management practices, more field work is required to properly quantify the contribution of the beef sector to regional NH_3 emissions. Airborne and ground-based measurements such as these, and improvements on the bLS model such as the inclusion of dry deposition in the next version, will indubitably be useful tools in this effort.

Acknowledgements

Foremost we acknowledge the help of our pilot Rob Buchanan, who perished tragically a few months after the study. We also thank Patrick Lee, Mohammed Wasey, Cris Mihele, Gang Lu, and Trevor Coates for assistance in the field.

References

Allan, J.D., Jimenez, J.L., Williams, P.I., Alfarra, M.R., Bower, K.N., Jayne, J.T., Coe, H., Worsnop, D.R., 2003. Quantitative sampling using an aerodyne mass spectrometer 1: techniques of data interpretation and error analysis. Journal of Geophysical Research 108, 4090. doi:10.1029/2002JD002358.

Allen, A.G., Harrison, R.M., Wake, M.T., 1988. A meso-scale study of the behaviour of atmospheric ammonia and ammonium. Atmospheric Environment 22, 1347–1353.

Aneja, V.P., Schlesinger, W.H., Niyogi, D., Jennings, G., Gilliam, W., Knighton, R.E., Duke, C.S., Blunden, J., Krishnan, S., 2006. Emerging national research needs for agricultural air quality. EOS Transactions 87 (3), 25.

Beig, G., Brasseur, G.P., 2000. Model of tropospheric ion composition: a first attempt. Journal of Geophysical Research 105, 22671–22684.

Berendse, F., Laurijsen, C., Okkerman, P., 1988. The acidifying effect of ammonia volatilized from farm manure on forest soils. Ecological Bulletin 39, 136–138.

Cheng, L., Angle, R.P., 1996. Model-calculated interannual variability of concentration, deposition and transboundary transport of anthropogenic sulphur and nitrogen in Alberta. Atmospheric Environment 30, 4021–4030.

Environment Canada, 2009. The 2008 Canadian Atmospheric Assessment of Agricultural Ammonia. Environment Canada, Gatineau, QC, Canada.

Flesch, T.K., Wilson, J.D., Yee, E., 1995. Backward-time Lagrangian stochastic dispersion models and their application to estimate gaseous emissions. Journal of Applied Meteorology 34, 1320–1332.

Flesch, T.K., Wilson, J.D., Harper, L.A., Crenna, B.P., 2005. Estimating gas emission from a farm using an inverse–dispersion technique. Atmospheric Environment 39, 4863–4874.

Flesch, T.K., Wilson, J.D., Harper, L.A., Todd, R.W., Cole, N.A., 2007. Determining ammonia emissions from cattle feedlot with an inverse dispersion technique. Agricultural and Forest Meteorology 144, 139–155.

Fowler, D., Pitcairn, C.E.R., Sutton, M.A., Flechard, C., Loubet, B., Coyle, M., Munro, R.C., 1998. The mass budget of atmospheric ammonia in woodland within 1 km of livestock buildings. Environmental Pollution 102 (S1), 343–348.

Georgii, H.W., Müller, W.J., 1974. On the distribution of ammonia in the middle and lower troposphere. Tellus 26, 180–184.

Hayden, K.L., Macdonald, A.M., Gong, W., Toom-Sauntry, D., Anlauf, K.G., Leithead, A., Li, S.-M., Leaitch, W.R., Noone, K, 2008. Cloud processing of nitrate. Journal of Geophysical Research, 113, D18201, doi:10.1029/2007JD009732.

Isermann, K., 1994. Agriculture's share in the emission of trace gases affecting the climate and some cause-oriented proposals for sufficiently reducing this share. Environmental Pollution 83, 95–111.

Jayne, J.T., Leard, D.C., Zhang, X., Davidovits, P., Smith, K.A., Kolb, C.E., Worsnop, D.R., 2000. Development of an aerosol mass spectrometer for size and composition analysis of submicron particles. Aerosol Science and Technology 33, 49–70.

Jimenez, J.L., Jayne, J.T., Shi, Q., Kolb, C.E., Worsnop, D.R., Yourshaw, I., Seinfeld, J.H., Flagan, R.C., Zhang, X., Smith, K.A., Morris, J., Davidovits, P., 2003. Ambient aerosol and sampling with an aerosol mass spectrometer. Journal of Geophysical Research 108 (D7), 8425. 781. doi:10.1029/2001JD001213.

Krupa, S.V., 2003. Effects of atmospheric ammonia (NH_3) on terrestrial vegetation: a review. Environmental Pollution 124, 179–221.

Laubach, J., Kelliher, F., 2005. Methane emissions from dairy cows: comparison of open-path laser measurement to profile-based technique. Agricultural and Forest Meteorology 135, 340–345.

Lemon, E., van Houtte, R., 1980. Ammonia exchange at the land surface. Agronomy Journal 72, 876–883.

Luebs, T.E., Davis, K.R., Laag, A.E., 1974. Diurnal fluctuation and movement of atmospheric ammonia and related gases from dairies. Journal of Environmental Quality 3 (3), 265–269.

McGinn, S.M., Janzen, H.H., Coates, T., 2003. Atmospheric ammonia, volatile fatty acids, and other odorants near beef feedlots. Journal of Environmental Quality 32, 1173–1182.

McGinn, S.M., Flesch, T.K., Harper, L., Beauchemin, K.A., 2006. An approach for measuring methane emissions from whole farms. Journal of Environmental Quality 35, 14–20.

McGinn, S.M., Flesch, T.K., Crenna, B.P., Beauchemin, K.A., Coates, T., 2007. Quantifying ammonia emissions from a cattle feedlot using a dispersion model. Journal of Environmental Quality 36, 1585–1590.

Roelofs, J.G.M., Kempers, A.J., Hondijk, A.L.F.M., Janssen, A.J., 1985. The effect of airborne ammonium sulphate on *Pinus nigra* var. *maritima* in the Netherlands. Plant and Soil 84, 45–56.

Ryden, J.C., McNeill, J.E., 1984. Application of the micrometeorological mass balance method to the determination of ammonia loss from a grazed sward. Journal of the Science of Food and Agriculture 35, 1297–1310.

Sommer, S.G., McGinn, S.M., Hao, X., Larney, F.J., 2004. Techniques for measuring gas emission from piled cattle manure. Atmospheric Environment 38, 4643–4652.

Toma and Bouma Management Consultants, 2006. Economic analysis of soil phosphorus limits on farms in Alberta. In: Alberta Soil Phosphorus Limits Project. Volume 4: Economics and Management. Alberta Agriculture, Food and Rural Development, Lethbridge, Alberta, Canada, 82 pp.

van der Eerden, L.J.M., 1982. Toxicity of ammonia to plants. Agricultural Environment 7, 223–235.
Wollenweber, B., Raven, J.A., 1993. Implications of N acquisition from atmospheric NH_3 for acid–base and cation–anion balance of *Lolium perenne*. Physiologia Plantarum 89, 519–523.
Zhang, L., Moran, M.D., Makar, P.A., Brook, J.R., Gong, S., 2002. Modelling gaseous dry deposition in AURAMS: a unified regional air-quality modelling system. Atmospheric Environment 36, 537–560.
Ziereis, H., Arnold, F., 1986. Gaseous ammonia and ammonium ions in the free troposphere. Nature 321, 503–505.